Quantitative T_1 Mapping and Oxygen Enhanced MRI in Patients with Interstitial Lung Disease

Kerry Hart[1,2], Helen Marshall[1], Neil Stewart[1], Martin Deppe[1], Steve Bianchi[3], Rob Ireland[2], Moira Whyte[4], David Kiely[3], and Jim Wild[1]

[1]Academic Unit of Radiology, University of Sheffield, Sheffield, United Kingdom, [2]Academic Unit of Clinical Oncology, University of Sheffield, Sheffield, United Kingdom, [3]Pulmonary Vascular Disease Unit, Royal Hallamshire Hospital, Sheffield, United Kingdom, [4]Academic Unit of Respiratory Medicine, University of Sheffield, Sheffield, United Kingdom

Introduction: Longitudinal relaxation mechanisms in the lung can be explained by interactions between free water molecules and those bound to macromolecules present in the matrix of the lung. Mapping the longitudinal relaxation time (T_1) of protons in lung tissue and blood can therefore provide information on disease induced parenchymal changes, with reduced lung T_1 values having been reported in the fibrotic human lung [1] and in patients with cystic fibrosis (CF) [2]. Moreover molecular oxygen dissolved in pulmonary blood and parenchyma shortens the T_1 depending upon the oxygen concentration and permits regional assessment of ventilation and oxygen diffusion from the alveoli into the lung capillaries [3]. The T_1 decrease under hyperoxic conditions has been shown to be reduced in CF [2], and reduced oxygen induced signal intensity changes in the lung have been reported in patients with interstitial lung disease (ILD) [4]. In patients with ILD the pulmonary interstitium becomes thickened, resulting in less efficient gas exchange. Idiopathic pulmonary fibrosis (IPF) causes progressive scarring of the lung tissue and Systemic Sclerosis (SSc) is an autoimmune disease where the connective tissues in the lung become thickened and fibrosed. Here quantitative T_1 mapping was performed in patients with IPF, patients with SSc and healthy volunteers under normal and oxygen enhanced (OE) hyperoxic conditions, and the imaging parameters were compared to other metrics of pulmonary gas exchange.

Methods: *T_1 Mapping Acquisition:* Six patients with IPF, six patients with SSc and eight healthy volunteers were scanned on a 1.5T whole body MRI system (GE HDx). Images were acquired using an inversion recovery Look-Locker imaging sequence consisting of a series of 16 small flip angle gradient echo readouts following a non-selective 180° pulse for spin preparation [5]. Sequence parameters were: TIs = 110-3194 ms, TE=1.0ms, TR = 3.1ms, α=7°, voxel size = 3.125x6.25x15 mm, one slice at the level of the descending aorta. Imaging was performed at expiratory breath-hold following inhalation of room air (10 acquisitions) and 100% oxygen (10 acquisitions) delivered at a rate of 15L/min. *T_1 Mapping Analysis:* Each set of imaging data were fitted pixel-by-pixel in Matlab according to the time-dependent signal intensities of the 16 constituent images, yielding a single quantitative T_1 map for each series of 16 T1s [6]. Mean T_1 maps were calculated for room air and 100% oxygen. ROIs were drawn in the whole right and whole left lungs, excluding the aorta in the latter, and the mean T_1 values over the ROIs measured. The difference between average baseline and oxygen enhanced T_1 maps on a pixel-by-pixel basis was used to map the magnitude of T_1 shortening under hyperoxic conditions (ΔT_1). Differences between IPF patients, SSc patients and healthy subjects were assessed using independent Mann-Whitney tests. *Correlations with Other Techniques:* ^{129}Xe chemical shift saturation recovery (CSSR) data [7] were acquired and fit to estimate alveolar septal thickness [8] in a subset of four IPF patients, six SSc patients and five healthy volunteers. Pulmonary function tests were performed in the same subset, including the diffusing capacity of the lung for carbon monoxide (DLCO). Correlations between T_1 mapping outputs and septal thickness and DLCO were assessed using Spearman's correlation coefficient (r).

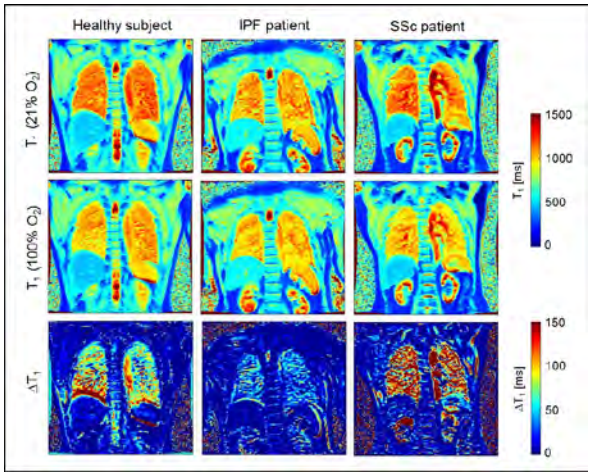

Figure 1: Example T_1 and ΔT_1 maps following inhalation of room air (21% oxygen) and 100% oxygen from a healthy volunteer, an IPF patient and a SSc patient.

Results and Discussion: Figure 1 shows example T_1 and ΔT_1 maps from a healthy volunteer, a patient with IPF and a patient with SSc. Baseline mean lung T_1 was significantly reduced in patients with IPF (p=0.005) and significantly reduced in patients with SSc (p=0.008) compared to healthy volunteers (fig 2a). Oxygen induced lung T_1 shortening was observed in all subjects and the magnitude of this shortening was significant for healthy volunteers (p<0.001), IPF patients (p<0.001) and SSc patients (p=0.001). Compared to healthy volunteers, mean lung ΔT_1 was significantly smaller in patients with IPF (p=0.003) (fig 2b). There was no significant difference in mean lung ΔT_1 between patients with SSc and healthy subjects (p=0.142). Strong significant correlations between baseline T_1 and septal thickness (r=-0.640, p=0.01) and between baseline T_1 and DLCO % predicted (r=0.652, p=0.008) were observed. Furthermore, ΔT_1 correlated significantly with septal thickness (r=-0.556, p=0.032) and with DLCO % predicted (r=0.562, p=0.029).

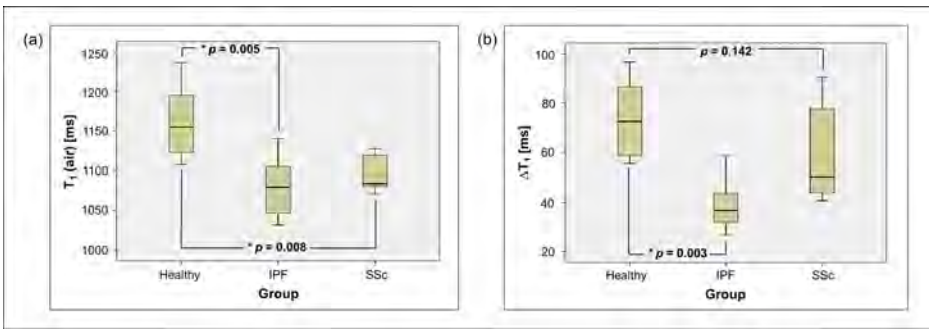

Figure 2: Mean (a) baseline lung T_1 values and (b) degree of oxygen induced T_1 shortening (ΔT_1) in healthy volunteers, IPF patients and SSc patients.

Conclusions: Quantitative T_1 mapping under normal oxygen concentrations demonstrated significantly reduced lung T_1 relaxation times in patients with IPF and SSc compared to healthy subjects, consistent with a higher proportion of fibrosed tissue per voxel in interstitial lung disease. The magnitude of T_1 shortening under hyperoxic conditions was shown to be significantly smaller in patients with IPF compared to healthy subjects, indicating reduced diffusion capacity and impaired oxygen transport in the fibrosed lung.

References: [1] Magn Reson Med 59:96-101 (2008); [2] Magn Reson Med 51:1009-1016 (2004); [3] Nature Medicine 2:1236-9 (1996); [4] J Magn Reson Imaging 26:1523-1529 (2007); [5] J Magn Reson Imaging 14:795-799 (2001); [6] J Magn Reson 96:608-612 (1992); [7] Magn Reson Med Epub (2014); [8] Magn Reson Med 69:884-890 (2013)